Journal of Electrical Bioimpedance
www.bioimpedance.net

J Electr Bioimp, vol. 6, pp. 18–21, 2015
Received: 1 Dec 2015, published: 11 Dec 2015
doi:10.5617/jeb.2571

Optically isolated current source

F. J. Pettersen[1,2,3] and J. O. Høgetveit[1,2]

[1] *Oslo University Hospital HF, Department of Clinical and Biomedical Engineering, Oslo, Norway*
[2] *University of Oslo, Department of Physics, Oslo, Norway*
[3] *E-mail any correspondence to: frepet@ous-hf.no*

Abstract

There is a need for isolated current sources for use in selected bioimpedance measurement circuits. The requirement for good isolation is particularly important in medical settings because of safety concerns. A new circuit for producing voltage-controlled current is presented. Measurements have been made on a prototype and simulations have been done on a SPICE model. The presented circuit is an H-bridge where the output devices are the output photodiodes of high-linearity optocouplers. Five operational amplifiers, four high linearity optocouplers, and passive components are used. Output current capability is $\pm 35\ \mu A$ with an output impedance that is more than $1\ M\Omega$. It is possible to achieve bandwidths above $1\ MHz$ for small load impedances. This circuit is well suited for medical applications thanks to the isolation in the optocouplers.

Keywords: Current source, isolation, optocoupler

Introduction

When making electrical impedance measurements, including bioimpedance measurements, electric impedance tomography (EIT), and focused impedance measurement (FIM), one or more electric currents are injected into the measurand. Depending on the application, one can choose to use a controlled voltage or a controlled current. For the cases where controlled current are used, it is important to have a well known current to be able to measure impedance or transfer-impedance accurately. To achieve this, one may use several different current sources that are already described such as [1–9].

An isolated current source is ideal to make independent current sources as required by FIM [10] since the outputs are independent of the inputs. In cases where measurements are done *in vivo*, regulations dictate a number of requirements [11]. One of these requirements is isolation of the measurand from the mains. The isolated current source presented here is made using devices that meet insulation requirements given in [11]. It is also important to limit the currents to avoid potential harmful effects such as unwanted muscle or nerve stimuli, including unintentional myocardial capture.

The isolated analog current sources available today are either transformer-coupled [3, 4] or optically coupled. Optical isolation is beneficiary since it allows operation to DC and is insensitive to electromagnetic fields. There are two main types of optically isolated current sources: The first is the use of one or more optocouplers to transfer a signal from the input to an opamp-based current source on the output side [8]. The second type is an H-bridge as presented in [9]. The current source presented here is of the second type. The novelty of the presented circuit is that it uses the optocouplers output currents directly. This is possible since linear optocouplers are used. Another important difference from other H-bridge circuits is that the presented circuit eliminates drift and nonlinearities due to aging or temperature.

Circuit

The optocoupler

This circuit is based on a particular type of optocoupler that is shown in figure 1. Necessary description to understand the presented circuit is as follows: The light emitting diode (LED) produces light that falls on two closely matched photodiodes, PD_1 and PD_2. This causes current to flow in the reverse direction in the photodiodes. The current gain from the LED to photodiode PD_1 is K_1 and the current gain from the LED to photodiode PD_2 is K_2. The ratio between the two current gains is $K_3 = \frac{K_2}{K_1}$. The factor K_3 will vary between different optocouplers, but a sorting is done by the manufacturers, and the final error must either be accepted, trimmed away, or a closer match must be found manually. Here, we assume that $K_3 = 1$. See data sheets [12, 13] and application notes [14, 15] for a complete description of the optocoupler.

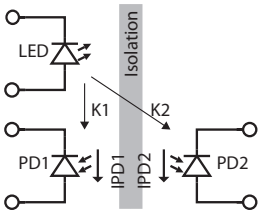

Fig. 1: The optocoupler.

Circuit description

The component, voltage, and current designators in this section refers to figure 2. To simplify, we define $R_1 = R_{1A} = R_{1B}$, $R_2 = R_{2A} = R_{2B}$, $R_3 = R_{3A} = R_{3B} = R_{3C} = R_{3D}$, $U_2 = U_{2A} = U_{2B} = U_{2C} = U_{2D}$, and $U_3 = U_{3A} = U_{3B} = U_{3C} = U_{3D}$

The circuit works as follows: The input signal is V_{IN}. The fully differential opamp U_1 and resistors R_{1A}, R_{1B}, R_{2A}, and R_{2B} convert this to a differential signal with an offset V_{Bias}. The signals on nodes A and B are then

$$V_A = -V_{IN} \cdot \frac{R_2}{R_1} + V_{Bias} \tag{1}$$

$$V_B = +V_{IN} \cdot \frac{R_2}{R_1} + V_{Bias} \tag{2}$$

These signals are then fed to the inputs of the four opamps driving the optocouplers as shown in figure 2. The optocoupler circuits convert the input voltages to currents in the output photodiodes. The gain in this step is given by

$$I_{PD2} = \frac{V_{[AorB]}}{R_3} \cdot K_3 \tag{3}$$

The currents flowing out of the optocouplers are now given by

$$I_{OUTA} = -V_{IN} \cdot G_1 + V_{Bias} \cdot G_2 \tag{4}$$

$$I_{OUTB} = +V_{IN} \cdot G_1 + V_{Bias} \cdot G_2 \tag{5}$$

where

$$G_1 = \frac{\frac{R_2}{R_1}}{R_3} \cdot K_3 \tag{6}$$

$$G_2 = \frac{1}{R_3} \cdot K_3 \tag{7}$$

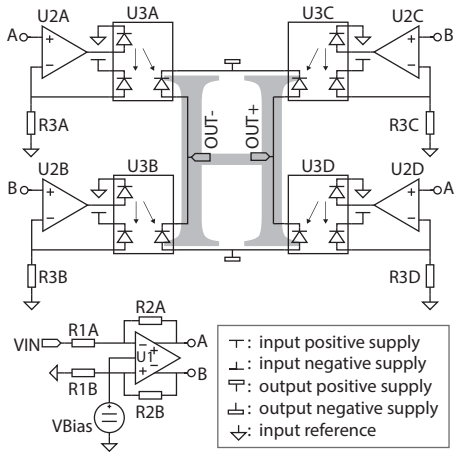

Fig. 2: The isolated H-bridge. The outputs A and B of the opamp-circuit at the bottom are the same nodes as A and B on the U_{2x} opamp inputs.

The optocouplers are connected so that when there is no input, i.e $V_{IN} = 0$, a bias current given by $\frac{V_{B1}}{R_3}$ will flow from U_{3A} to U_{3B} and from U_{3C} to U_{3D}. The net current flowing out of $OUT+$ or $OUT-$ is zero. When an input signal is present, there will be a current flowing out of $OUT+$ given by

$$I_{OUT+} = I_{OUTB} - I_{OUTA} = +V_{IN} \cdot G_1 \tag{8}$$

$$I_{OUT-} = I_{OUTA} - I_{OUTB} = -V_{IN} \cdot G_1 \tag{9}$$

The power supplies for the input are balanced regulated supplies (both positive and negative supply) of equal magnitude. The power supplies for the output should have the same voltage difference from positive to negative supplies as the power supplies on the input to ensure as similar conditions for PD_1 and PD_2 as possible. The supplies on the input and output can be separated for medical safety.

The maximum photodiode current is approximately 87 μA [12,13], which enables us to work with a bias current of up to 40 μA plus a signal up to 35 μA. This means that each current branch can be modeled as a current source that delivers up to ± 35 μA in parallel with an output impedance.

Figure 2 does not show all details of the circuit creating the differential signal or the bias circuit as this is regarded as outside the scope of this article. The details of the circuits driving the optocoupler is also left out as this information can be found in [12, 14, 15].

If we assume that the amplifier made of U_1, R_1, and R_2 can be made significantly faster than the rest of the circuit, we have two parts that limit the bandwidth of this circuit. The first part is the feedback loop made of U_2, $U_3 - LED$, $U_3 - PD_1$, and R_3. If we choose an opamp that is capable of driving $U_3 - LED$ significantly faster than the desired bandwidth, we end up with the node at the anode of $U_3 - PD_1$ as the dominant pole. The capacitance at this node is the combination of the parasitic capacitances in $U_3 - PD_1$ and U_2. This capacitance forms an RC-section together with R_3, which limits the speed. Depending on signal swing, we may have a slew-rate limitation since the current from the photodiode is very limited. The second part that limits the bandwidth is the output circuit. This circuit is essentially a controlled current source in parallell with the parasitic capacitances from $U_3 - PD_2$. If we assume a pure resistive load, the bandwidth is limited by the pole formed of the capacitance and the load. As for the first part, this part may also suffer from slew-rate limitations. The output impedance is thus $\frac{1}{j\omega C_O}$ where C_O is the parasitic capacitance seen at the output node.

Two variants of the prototype was made, with different opamps. The opamps had different Gain-Bandwidth (GBW). The first featured an opamp with $GBW = 1.7$ MHz and the second an opamp with $GBW = 4$ MHz. Output impedance was found for several frequencies, and -3 dB-bandwidth was found for both opamp-variants. In addition, a SPICE model was made and simulated.

The datasheet for the optocoupler or the SPICE model do not give necessary data to calculate the output impedance accurately, but the data available suggest output impedances in the range 10 $M\Omega$ or more.

Noise

The output noise of this circuit is dependent on noise contributions from all devices and on the frequency dependent transfer function to the output. We have not made a generic noise analysis that is including all noise sources due to the high complexity in such calculations. Instead we have made a simplified noise analysis. The simplified noise analysis is shown in equation 10. This is a noise analysis where U_1, U_2, and U_3 is assumed to be noiseless, and K_3 is assumed to be 1.

$$i_{noise}^2 = G_1^2 v_{nR1}^2 + G_2^2 \left(v_{nR2}^2 + 4 v_{nR3}^2 \right) \quad (10)$$

The noises are calculated using equation 11 where k_B is the Boltzmann constant and T is the temperature in Kelvin.

$$v_{nRX} = \sqrt{4 k_B T R} \quad (11)$$

Equations 10 and 11 show us that if the resistance in R_3 is higher or comparable to that of R_2, then the noise from R_3 dominates. The resistances R_1 and R_2 can easily be set to values significantly lower than that of R_3. We may set $R_1 = R_2$, which let us simplify equation 10 to

$$i_{noise}^2 = \frac{16 k_B T}{R_3}. \quad (12)$$

Measurement and simulation results

The measured output impedance is shown in figure 3.

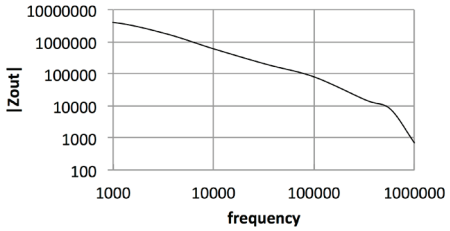

Fig. 3: Output impedance (Ω) versus frequency (Hz).

Simulations of the circuit with different opamps gave results shown in table 1.

Tab. 1: Measured and simulated bandwidths, unit for all parameters is MHz.

Opamp	*Opamp GBW*	*Sim. or Meas.*	*BW*
TLC274	1.7	Measured	0.68
TLC274	1.7	Simulated	1.28
TS924	4	Measured	1.35
TS924	4	Simulated	2.42
LT1214	28	Simulated	6.90

TLC274 is from Texas Instruments, TS924 is from ST Microelectronics, and LT1214 is from Linear Technology.

Discussion

The data sheet for the Avago Technology optocoupler states that the LED bandwidth is 9 MHz, which confirms that the LED is not limiting the bandwidth. The same data sheet also states that the bandwidth for the optocoupler is 1.5 MHz, which may indicate that the maximum bandwidth in the circuits presented in [12] and [15] have a 1.5 MHz limitation and that the circuit presented here may actually have higher bandwidth, or it may indicate that the SPICE model in [12] is not good enough to model limitations in the optocoupler.

We have demonstrated that it is feasible to operate the circuit up to 1.35 MHz. If we look at the simulated performance, we see that simulated bandwidth is approximately 1.8 times higher than the measured, which indicates that the model is not perfect. But even if the SPICE model is not perfect, it clearly indicates that it may be possible to increase bandwidth even further. If the ratio of 1.8 for simulated versus measured bandwidth is valid for all simulations and if the optocoupler model is valid, we could expect a bandwidth of 3.8 MHz if we used the LT1214, which is 2.5 times higher than the data sheet for the optocoupler suggests.

Optimization of bandwidth means choosing opamp U_2 that is fast and powerful enough to drive the LED, and that does not contribute too much to the parasitic capacitance to the node at the anode of $U_3 - PD_1$, and a proper choise of R_3.

Bandwidth as high as the presented circuit is capable of can be useful for electrical bioimpedance measurements, including bioimpedance spectroscopy.

The presented circuit has the potential to outperform the noise performance of other circuits based on linear optocouplers since it uses an absolute minimum of noise-contributing components on the output side. By careful design, the main noise contributor will be R_3, which is determined by available voltage swings, bandwidth requirements, and required output current. The opamps and optocouplers are considered noiseless in equation 10, which means that the noise-model will underestimate the noise. The contribution from the optocouplers is not known, and the contribution from the opamps will be very variable depending on the opamps used. The SPICE model for the optocoupler does not include noise sources [12]. If noise is a concern, a thorough noise analysis or simulation should be done, but this will require an optocoupler model that models noise.

There are a number of alternatives that have not been explored since this article is only aiming to present the basic idea for the new circuit. Examples of alternatives are: Use of only one output branch, automatic adjustment of cancel mismatch in the optocouplers, several sources driven by U_1, or to switch off the bias current when the circuit is not active.

The optocouplers are used in photoconductive mode, which requires supplies on the output side. One could also use the optocouplers in photovoltaic mode to eliminate the need for a supply on the output side, but the available energy is very limited, so the bandwidth would be low.

Conclusion

The presented circuit is a galvanically isolated voltage controlled current source. It is made using linear optocouplers with an absolute minimum of components in the isolated output section. Thanks to no components on the output side, the circuit has potential for low noise. The isolation makes it suitable for use in medical purposes such as bioimpedance, FIM, EIT, or nerve stimulation.

References

1. D. H. Sheingold. Impedance & admittance transformations using operational amplifiers. *The Lightning Emiricist*, 12(1), 1964.

2. R. Bragós, J. Rosell, and P. Riu. A wide-band ac-coupled current source for electrical impedance tomography. *Physiological measurement*, 15 Suppl 2:A91–9, 1994. http://dx.doi.org/10.1088/0967-3334/15/2A/013

3. K. G. Boone and D. S. Holder. Current approaches to analogue instrumentation design in electrical impedance tomography. *Physiological measurement*, 17(4):229–47, 1996. http://dx.doi.org/10.1088/0967-3334/17/4/001

4. H. G. Goovaerts, Th J. C. Faes, E. Raajimakers, and R. M. Heethaar. An electrically isolated balanced wideband current source: basic considerations and design. *Medical & Biological Engineering & Computing*, 36(5):598–603, 1998. http://dx.doi.org/10.1007/BF02524430

5. Alex Birkett. Bipolar current source maintains high output impedance at high frequencies. *Electronic Design News*, pages 128–130, December 2005.

6. M. Rafiei-Naeini and H. McCann. Low-noise current excitation sub-system for medical eit. *Physiological measurement*, 29(6):S173–84, 2008. http://dx.doi.org/10.1088/0967-3334/29/6/S15

7. Uwe Pliquett, Markus Schönfeldt, Andreas Barthel, Dieter Frense, Thomas Nacke, and Dieter Beckmann. Front end with offset-free symmetrical current source optimized for time domain impedance spectroscopy. *Physiological measurement*, 32(7):927–44, 2011. http://dx.doi.org/10.1088/0967-3334/32/7/S15

8. E. Borges, E. Figueiras, H. C. Pereira, J. M. Cardoso, L. R. Ferreira, and C. Correia. Optically isolated current source. *IFMBE Proceedings*, 25/4:2020–2023, 2010. http://dx.doi.org/10.1007/978-3-642-03882-2_536

9. D. Prutchi and M. Norris. *Design and Development of Medical Electronic Instrumentation: A Practical Perspective of the Design, Construction, and Test of Medical Devices*. Wiley, 2005.

10. K. S. Rabbani, M. Sarker, M. H. R. Akond, and T. Akter. Focused impedance measurement (fim): A new technique with improved zone localization. *Annals of the New York Academy of Sciences*, 873(1):408–420, 1999. http://dx.doi.org/10.1111/j.1749-6632.1999.tb09490.x

11. IEC 60601-1 - medical electrical equipment - part 1: General requirements for basic safety and essential performance, 2013.

12. Avago Technologies. Hcnr200 and hcnr201 high-linearity analog optocouplers, 2011.

13. Vishay Semiconductors. Linear optocoupler for optical data in telecommunications, high performance, Nov. 9, 2012.

14. Bob Krause. Designing linear amplifiers using the il300 optocoupler appnote 50, 1996.

15. Avago Technologies. Overview of high performance analog optocouplers, application note 1357, Aug. 2, 2011.